Extended Sub-sampling in OFDM Environment

Nikos Petrellis
Computer Science and Engineering Dept.
TEI of Thessaly
Larissa, Greece
npetrellis@teilar.gr

***Abstract*— The sub-sampling method for Orthogonal Frequency Division Multiplexing (OFDM) that has been recently proposed by the author, is extended in this paper allowing the Analog-to-Digital Converter (ADC) of the receiver to operate in low power mode, up to ¾ of the time. The predictability of the parity patterns generated by the Forward Error Correction encoder (FEC) of the transmitter when it accepts as input sparse data is exploited in order to define appropriate Inverse Fast Fourier Transform (I-FFT) input symbol arrangements. These symbol structures allow the substitution of a number samples by others that are already available on the receiver side. Moreover, several FFT and IFFT operations can be deactivated because they output zeros when they accept as input a number of identical values. The advantages of the proposed method are: low power, higher speed, fewer memory resources and most importantly implementation with very low cost hardware. The simulation results show that full input signal recovery or at least a very low Bit Error Rate (BER) in the order of 10^{-4} is possible in most of the cases that have been tested.**

Keywords—OFDM, Sub-sampling, ADC, Low Power, FFT, FEC

I. INTRODUCTION

The sub-sampling method presented in this paper is an extension of the work described [1] and [2]. A signal can be reconstructed from fewer samples than those required by the Nyquist theorem using methods like Compressive Sampling (CS), Kalman filters, interpolation, etc. Some of these approaches are briefly described in order to examine their implementation complexity and their performance compared to the proposed method. Fewer samples can be used if the information exchanged is sparse or compressible and in this case a sampling rate close to the actual information rate can be used [3]. The CS techniques are based on optimization problems that are solved using iterative methods [4]. The hardware implementation of a CS algorithm can be performed using reconfigurable hardware [5] or DSP processors [6].

In [7] images with 32×32 pixels have been used and the Normalized Mean Square Error (N-MSE) achieved in various configurations ranges between 0.11 and 0.86. CS techniques applied for face recognition are described in [8]. Radar data recovery using CS techniques is discussed in [9]. The simulation results show that the NMSE ranges between 1.5 and 2.5 when radar images are reconstructed with the Signal to Noise Ratio (SNR) being between -5dB and 4dB. In [10] a CS technique is applied to underwater sensor network. The data are expressed as sparse coefficients of a DFT and 99% of the energy is concentrated in 13 of the 200 coefficients.

Signal correction can also be based on Kalman filters as in [11] where the MSE ranges between 10 and 22 in some of the examined cases and is reduced below 0.2 under specific conditions. In [12], the least square CS approach is described and Discrete Wavelet Transform coefficients are used. A cardiac image sequence with 35% measurements is tested. The NMSE measured was approximately 10^{-2}. In [13], the CS problem is solved as a Kalman filter and the MSE measured is approximately 0.5 in the various cases studied while it tends to 0 in some cases (4% sparseness degree). The channel estimation in OFDM environments can be handled as a CS problem. The NMSE in [14] is lower than 10^{-5} when SNR=50dB and in [15], the BER that refers to the pilots can be as low as 0.5×10^{-3} when SNR=11dB.

In the work presented in this paper, the sub-sampling mode allows the operation of the ADC in lower power since its consumption is proportional to its sampling rate [16]. The memory requirements, the speed and the power consumption of the transmitter IFFT and the receiver FFT are also reduced. The proposed information recovery method exploits the data sparseness in time domain and the predictability of the parity bit pattern at the output of the transmitter FEC encoder when its input is sparse. The symbols at the transmitter IFFT input are arranged appropriately so that the reconstruction of the information from fewer samples is possible on the receiver side. The receiver ADC provides only the necessary samples and copies of these, are used to prepare the receiver FFT input. Some IFFT/FFT butterfly outputs can also be predicted and thus, the deactivation of many FFT operations is possible saving time and power. General OFDM infrastructures can benefit from the proposed system during the exchange of occasionally sparse information. It can also be used in systems that sparsify the initially non sparse data by using the differences of successive samples or by setting to zero samples with small value. The origin of the sparse data can be large sensor networks, surveillance cameras, traffic control sensors, etc. Compressed data can be transmitted over the proposed OFDM system and power can still be saved during the pause intervals between successive sessions.

This work is different from [1] in that the maximum theoretical number of samples that can be omitted from the sub-sampling procedure is increased by 50%. Several different

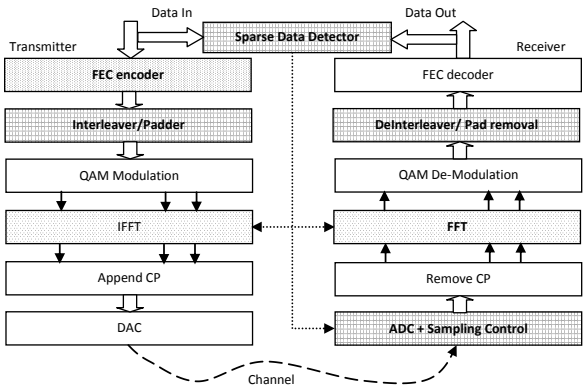

Figure 1. Architecture of the OFDM Transceiver.

IFFT input symbol arrangements are introduced and tested while the exact IFFT/FFT operations that can be deactivated are described in detail. Different simulations than [1] and [2] are used to show the effect of these IFFT/FFT modifications. The limitations concerning the value of the padding and the pilot symbols have been removed in this work. In this work presented the exact IFFT/FFT operations that can be omitted are described in detail (there is no similar analysis in the [1] and [2]).

This paper is organized as follows: the architecture of the OFDM systems and the exploited DFT properties are described in Section 2. Appropriate IFFT input symbol arrangements are described in Section 3. The description of the IFFT/FFT operations that can be deactivated are presented in Section 4. The simulation results are discussed in Section 5.

II. OFDM Architecture – Undersampling Method

The OFDM systems are based on the digital modulation of orthogonal carriers. The block diagram describing the OFDM transmitter and receiver architecture is shown in Fig. 1. The input data bits at the transmitter are used by the FEC encoder in order to generate the parity bits. Then, the data and the parity bits are interleaved (to avoid burst errors) and mapped to symbol constellations like q-order Quadrature Amplitude Modulation (q-QAM). The modulated symbols X_k with $0 \le k < N$, form the input of an N-point IFFT that generates the complex time symbols x_n with $0 \le n < N$. The x_n symbols are sequentially transmitted over the communication channel after

Figure 2. The employed RSC Encoder.

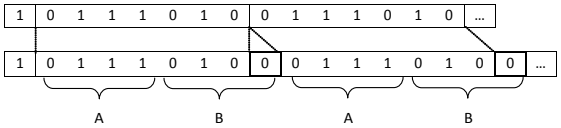

Figure 3. Parity Patterns generated after the first '1' at the encoder input of Fig. 2 before and after the padding (top and bottom respectively).

appending a Cyclic Prefix (CP) in order to avoid Inter-Symbol Interference. The reverse procedure has to be followed at the receiver. The N complex y_n symbols are generated from the ADC and form the input of the N-point FFT that generates the symbols Y_k. The symbols Y_k are mapped to the closest q-QAM constellation and demodulated in order to generate the data and parity bit stream. This bit stream is de-interleaved and decoded by an appropriate FEC method like Viterbi, Turbo decoding, etc.

A typical architecture of a Recursive Systematic Convolutional (RSC) FEC encoder is shown in Fig. 2 and this specific encoder is used in the architecture described in the rest of this paper. Its Systematic output is connected to the data input. The feed forward and the feedback paths of Fig. 2, determine the parity output and are characterized by the polynomials $1+D+D^2+D^3$ and $1+D+D^2$ respectively (D^p denotes a delay of p encoder clock periods). The parity output generates the redundant bit used for error correction at the receiver. Although the data and the parity bits are often driven into the interleaver in an alternating manner, it has to be guaranteed here, that the QAM symbols will be generated either from parity or data bits only using buffering.

The parity output of an encoder like the one of Fig. 2 remains '0' as long as the input is '0'. When a single '1' enters the encoder input, a repeated l-bit parity pattern is generated at the output until a second '1' appears at the input. Then, a different parity pattern is generated repeatedly until a third '1' appears and so on. The length l of these repeated parity patterns, depends on the Trellis decoding diagram of

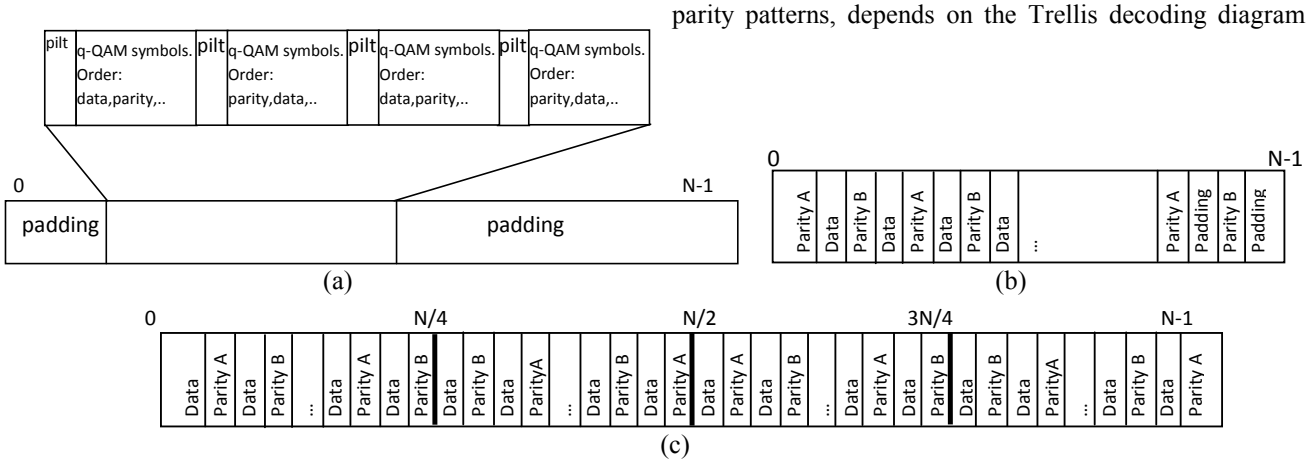

Figure 4. IFFT Input Symbol Arrangements (PS0) was used in [1] (a), IFFT Input Symbol Arrangements used in this Work: PS1 (b), PS2 (c).

the RSC FEC encoder [16]. The length *l* of the Fig. 2 encoder is 7. The 7-bit pattern that is generated by the encoder of Fig. 2, between the first two 1's is shown at the top of Fig. 3. These repeated 7-bit patterns can be mapped directly to a QAM symbol if 128-QAM is used. If 16-QAM is used instead, a padding with a '0' bit can be used at the end of each 7-bit parity pattern in order to generate a pair of 16-QAM parity symbols (denoted as A and B) with predictable value (bottom of Fig. 3).

The bit-interleaver is allowed to permute data and parity bits provided that each q-QAM symbol is generated either from data or parity bits only. The generated data or parity q-QAM symbols are arranged at the IFFT input as will be described in the next section. The form of the IFFT input packet and the sparseness level of the data, allow the replacement of some y_n symbols by others that have probably equal value at the receiver. Thus, the ADC can operate at lower sampling rate (sub-sampling mode) during specific time intervals leading to power consumption reduction. Some IFFT/FFT operations can also be skipped as will be explained in the next section.

A sparseness detector can be used in both the OFDM transmitter and receiver in order to control the sub-sampling process and the deactivation of IFFT/FFT operations. Such a detector can be implemented as a counter of zeros at the input of the transmitter and the output of the receiver. A large sequence of zeros indicates that sparse data are exchanged while the end of this period can be signaled by the occurrence of too many errors.

The definition of the Inverse Discrete Fourier Transform (IDFT) for x_n and $x_{n+N/2}$ with n odd, can be written as:

$$x_n = \frac{1}{N}\left(\sum_{k=0,2,\ldots}^{N-2} X_k w_N^{kn} + \sum_{k=1,3,\ldots}^{\frac{N}{2}-1} (X_k - X_{k+\frac{N}{2}}) w_N^{kn}\right) \quad (1)$$

$$x_{n+\frac{N}{2}} = \frac{1}{N}\left(\sum_{k=0,2,\ldots}^{N-2} X_k w_N^{kn} - \sum_{k=1,3,\ldots}^{\frac{N}{2}-1} (X_k - X_{k+\frac{N}{2}}) w_N^{kn}\right) \quad (2)$$

where the twiddle factors w_N^r are defined as $w_N^r = e^{i2\pi r/N}$. The second sum in (1) and (2) equals to 0, if $X_k = X_{k+\frac{N}{2}}, \forall k < \frac{N}{2}$, with k odd. In this case: $x_n = x_{n+\frac{N}{2}}$ for odd n values. This condition is satisfied if all the data X_k, pad and pilot symbols that have been placed at odd k positions are equal. If the data X_k symbols have been derived by sparse data, then most of their values will be indeed equal while if the pad and pilot symbols used in the odd positions are also selected with the same value, it can be assumed that x_n is equal to $x_{n+\frac{N}{2}}$ for odd n values. The sub-sampling approach of [1] has been based on this principle (50% sub-sampling).

In this work, we also take into consideration that many successive parity X_k symbol pairs can also have identical value if the parity prediction/padding method described earlier is followed. If R is the number of x_n values that are substituted by others, then R can be up to N/4 (half of the x_n with odd n) in [1]. Of course, some X_k symbols are not equal to $X_{k+\frac{N}{2}}$ (with odd *k)* since the input data are sparse but some data X_k symbols do not have trivial value. A lower error can be achieved if R is low, since fewer symbols are replaced by others with different value in this case.

The IDFT can be expressed as follows if we focus on the x_n with odd n and $n<N/2$:

$$\begin{aligned} x_n = &\Big(\sum_{k=1,3,..,\frac{N}{4}} (X_k w_N^{kn} - X_{\frac{N}{2}-k} w_N^{-kn}) + \\ &\sum_{k=1,3,..,\frac{N}{4}} (-X_{k+\frac{N}{2}} w_N^{kn} + X_{N-k} w_N^{-kn}) \\ &+ \sum_{k=2,..,\frac{N}{2}-2} (X_k w_N^{kn} + X_{N-k} w_N^{-kn}) + X_0 - X_{\frac{N}{2}}\Big)\frac{1}{N} = x_{\frac{N}{2}-1} \end{aligned} \quad (3)$$

In equation (3) it has been taken into consideration that $w_N^{n(\frac{N}{2}-k)} = -w_N^{-nk}$, $w_N^{n(\frac{N}{2}+k)} = -w_N^{nk}$ and $w_N^{n(N-k)} = w_N^{-nk}$. The first sum in equation (3) adds the X_k pairs at odd positions that are symmetric around N/4, the second sum adds the X_k pairs with odd k, that are symmetric around 3N/4 and the last sum adds the X_k pairs with even k, that are symmetric around N/2.

It can be stated that the IFFT outputs x_n and $x_{\frac{N}{2}-n}$ are equal (n<N/2), if: (a) $X_k = X_{\frac{N}{2}-k}$ (with odd k and k≤N/4), (b) $X_{k+\frac{N}{2}} = X_{N-k}$ (with odd k and k≤N/4) and (c) $X_k = X_{N-k}$ with even k and 0≤k<N/2. This can also be proved in a similar way for x_n and x_{N-n}, if n is odd and N/2<n<3N/4.

The conditions (a)-(c) defined above can be used to extend the lower sampling rate interval by 50% and thus the maximum R value from N/4 to 3N/8 (75% sub-sampling mode).

III. IFFT Input Symbol Arrangements

Fig. 4a shows the IFFT input symbol arrangement (denoted as PS0) used in [1]. In PS0 all the odd positions are mapped to data, pad or pilot X_k symbols that are assumed to be equal to a common value X_c. The order of the data and parity symbols is reversed following a pilot symbol. In this way, X_c values are expected in all the odd positions of the packet payload. The new input symbol arrangements of Fig. 4b and 4c have been used in this paper. The padding symbols shown in Fig. 4a, normally appear only in the last IFFT input packet of a communication session and do not need to be considered for every IFFT input packet. The sub-carriers that are dedicated for padding can also be used for pilots. If pilots are used in the place of data symbols then, if their value is selected to be equal to X_c then, no additional error is expected.

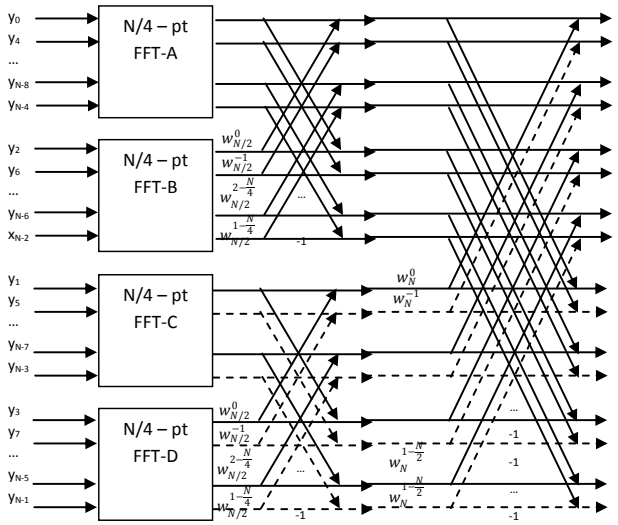

Figure 5. The FFT Implementation.

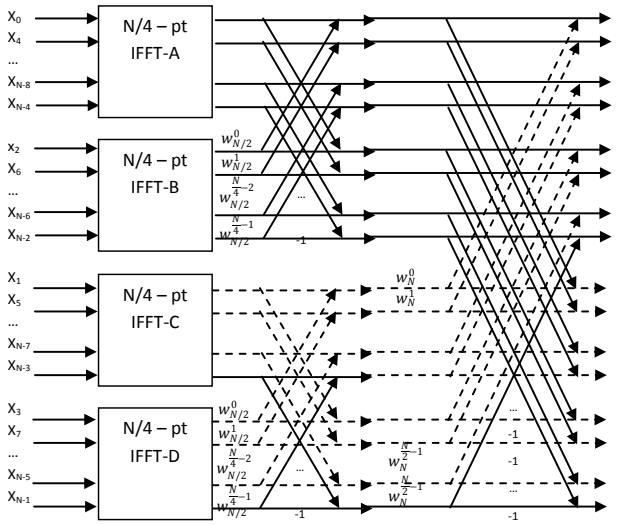

Figure 6. The IFFT Implementation.

Using pilots with a different value than X_c in the place of data symbols, results in worse error in the same way as if the sparseness level of the input data was worse. The pilots can also be placed at the position of parity symbols and in this case either some parity symbols have to be punctured or the data payload length should be adjusted appropriately in order to fit the data, the pilots and all the necessary parity symbols in the IFFT input packet.

In the case of the PS1 structure that appears in Fig. 4b, the data QAM symbols have been placed at the odd positions and the same holds for the N/16 data padding symbols X_c at the end of the packet. In this symbol arrangement the 50% sub-sampling scheme can be followed.

The conditions (a)-(c) of the previous section can be satisfied if the IFFT input symbol arrangement of Fig. 4c is used (PS2). In this case the 75% sub-sampling mode can be used. The data symbols have been placed at the even positions while the parity symbols have been placed in symmetric positions around N/4 and 3N/4. It is important that the parity symbols are scattered in an alternating manner around N/4, and 3N/4. If they are successively placed from the start of the packet towards its end, the conditions (a)-(b) of the previous section would not be valid. Consider for example the case where, 3/4 of the parity symbols are A1 and B1 and the rest of them A2 and B2. A1 is placed at the positions 1, N/2-1, N/2+1, N-1 and then at the positions 5, N/2-5, N/2+5, N-5 and so on. Then parity symbols B1 would have been placed at the positions 3, N/2-3, N/2+3, N-3, then at the positions 7, N/2-7, N/2+7, N-7, etc. The conditions (a) and (b) of the previous section are usable in this case. However, if these symbols had been placed sequentially from the start of the packet, the symmetric symbols around 3N/4 would be A1 and A2 (or B1 and B2) and the condition (b) would be invalid.

IV. Modified IFFT/FFT Operation

This FFT implementation by Cooley and Tukey [17] avoids the calculation of the same parameters multiple times. In the simplest case a radix-2 FFT corresponds to an N-point FFT that is constructed by a pair of N/2 point FFTs interconnected as a "butterfly" (see Fig. 5). One of these N/2-point FFTs accepts as input the odd positioned symbols of the N-point FFT and the other accepts as input the symbols from the even positioned global inputs. Each one of these N/2 point FFTs can be recursively implemented by a pair of N/4-point FFTs and this process can be repeated until 2 point FFTs are defined. The definition of the N-point DFT requires N^2 operations that are reduced to $N \cdot \log_2 N$ using this FFT implementation. The inputs in the FFT sub-blocks are bit reversed while the outputs are in normal order. If R is selected equal to N/4 in the sub-sampling mode described in the previous sections, then all the input pairs of the N/4-point, FFT-C or D of Fig. 5 with distance N/8 are equal (N/4 of the odd-positioned FFT inputs $y_{n+N/2}$ (n<N/2) have been substituted by y_n). If every N-point FFT input value appears twice, then half of the FFT output values (the ones at odd-k positions) will be zero according to the following expression:

$$Y_k = \sum_{n=0}^{N/2-1} y_n w_N^{-kn} + \sum_{n=0}^{N/2-1} y_{n+\frac{N}{2}} w_N^{-k(n+N/2)}$$
$$= \sum_{n=0}^{N/2-1} y_n w_N^{-kn} + (-1)^k \sum_{n=0}^{N/2-1} y_n w_N^{-kn} \quad (4)$$

The dashed outputs of the FFT-C and FFT-D sub-blocks in Fig. 5 correspond to zero outputs of these N/4-point FFTs and the operations that use these zero values as inputs can be omitted. Of course, similar operations can be deactivated in the hidden blocks within the N/4-point FFTs. More specifically, the number of FFT multiplications and additions that can be omitted if R=N/4, is 3/8. If R=N/8 then FFT-D only will have all the odd positioned outputs zero. In this case, 1/8 of the additions and multiplications can be omitted.

The IFFT on the transmitter side can be implemented with a similar configurable architecture as shown in Fig. 6. If the IFFT input symbol arrangements PS0 or PS1 are employed, the QAM symbols that are placed in the odd positions are expected to have identical values (X_c). If all the inputs of an IFFT are equal to X_c, then the x_0 output of the IFFT is equal to

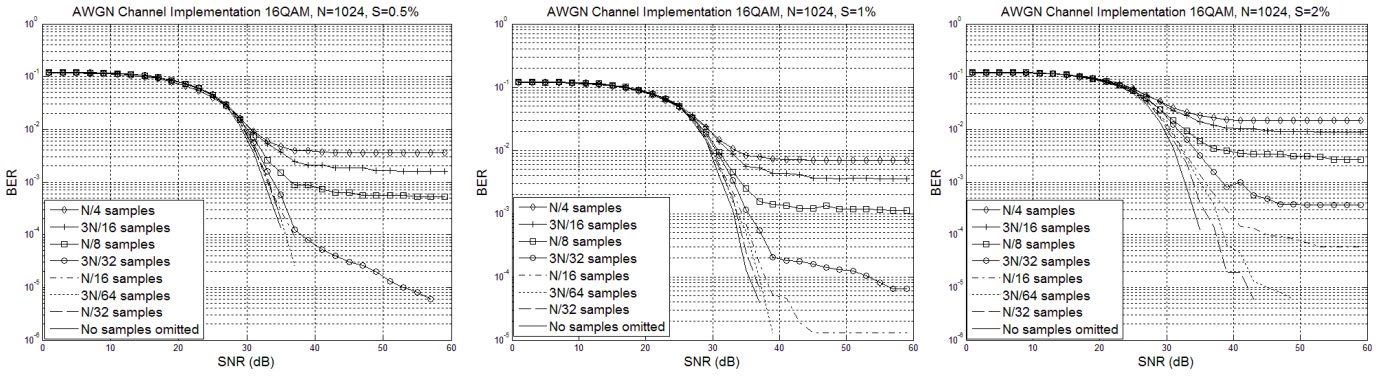

(a) (b) (c)

Figure 7. OFDM with AWGN Channel, PS2, N=1024, 16-QAM Modulation and S=0.5% (a), S=1% (b), S=2% (c).

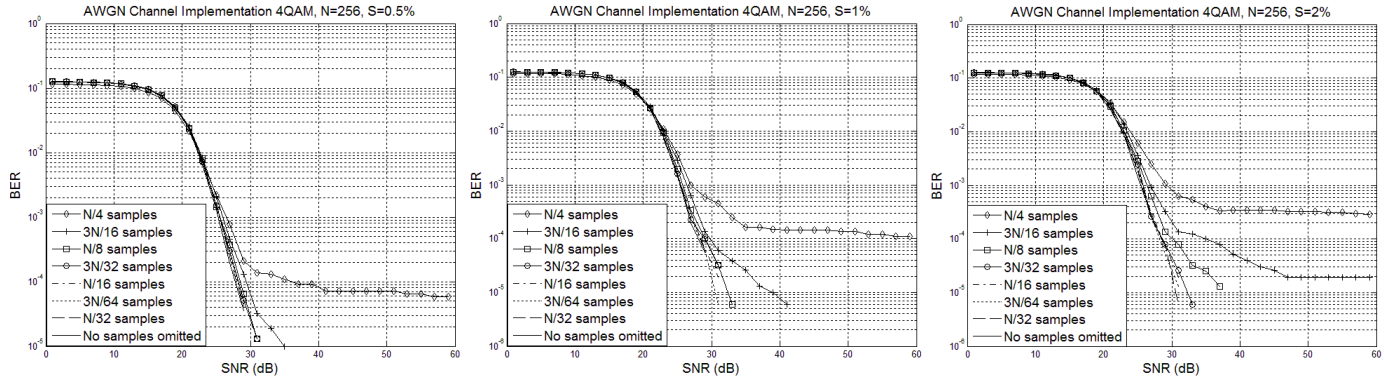

(a) (b) (c)

Figure 8. OFDM with AWGN Channel, PS2, N=256, 4-QAM Modulation and S=0.5% (a), S=1% (b), S=2% (c).

X_c and all the other outputs are 0 since:

$$x_n = X_c \frac{1}{N} \sum_{n=0}^{N-1} w_N^{kn} = 0 \quad ,n\neq 0 \tag{5}$$

$$x_0 = \frac{X_c}{N} \sum_{k=0}^{N-1} w_N^{k0} = X_c \tag{6}$$

The dashed lines at the outputs of the N/2-point IFFT at the bottom of Fig. 6 denote that they are all zero except from the output No. 0. The IFFT sub-blocks (with size < N/2) can be turned off during the sub-sampling period with a slight error overhead since most of the X_k values have identical values but a few of them will be inevitably different than X_c. A lower error is expected if IFFT sub-blocks with smaller size are turned off.

V. Simulation Results - Discussion

The simulation of an OFDM system with an AWGN channel was carried out for two combinations of N and q: N=1024, q=16 (Fig. 7) and N=256, q=4 (Fig. 8). The sparseness levels S tested were 0.5%, 1% or 2%. The number R of replaced y_n samples was: N/4, N/8, N/16, N/32 (50% sub-sampling mode) and 3N/16, 3N/32, 3N/64, or N/32 (75% sub-sampling mode). The case where no sub-sampling is performed is also included as a reference. The packet structure used for the input of the IFFT is the PS2 that is compliant with the conditions (a)-(c) of Section II. As can be seen from the simulations of Fig. 7 and 8 a lower BER can be achieved if low R, S, N values and low order QAM modulation are used. The combination 4-QAM (QPSK) and N=256 leads to the best BER since a full reconstruction is always possible at least if S=0.5% or S=1%. When S=2% a low error floor appears when R=N/4 (approximately 10^{-4}) and when R=3N/16 (close to 10^{-5}).

In Fig. 9 the OFDM system with N=1024 and 16-QAM modulation is used to test the effect of FFT/IFFT operation deactivation. The number of substituted samples is R=N/8 and thus, deactivating the appropriate N/8-point FFT sub-bock, should not affect the error. Nevertheless, larger FFT/IFFT sub-blocks are also turned off in the simulations to measure the effect of this deactivation on the achieved BER. If full IFFT and FFT implementation is used, a BER error floor close to 10^{-4} and 10^{-5} appears respectively. The tested cases include the following: (a) no deactivation (full FFT/IFFT implementation), (b) N/4-point FFT, (c) N/2-point FFT, (d) N/4-point IFFT and (e) N/2-point IFFT.

The simulations of Fig. 9 were conducted using the PS1 IFFT input symbol arrangement of Fig. 4c. Had PS2 been used instead, worse results would have been obtained. This is due to the fact that the deactivated FFT/IFFT sub-blocks are the ones with the odd-positioned inputs and the PS1 structure has mapped data symbols to the odd positions while the PS2 structure has mapped parity symbols there. Although almost all of the data symbols have identical value (X_c), the parity symbols don't. If the deactivated FFT/IFFT sub-blocks were the ones with the even positioned inputs the results would

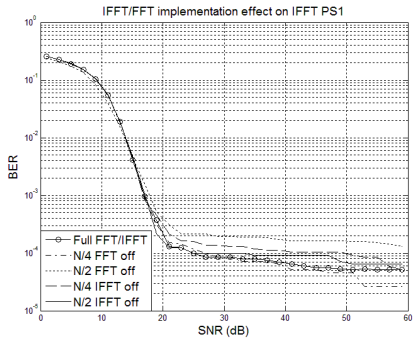

Figure 9. The Effect of Deactivating FFT/IFFT Operations to the BER of an OFDM System with N=1024, 16-QAM and PS1

have been reversed and the PS2 would show better performance than PS1. The BER is affected more by the deactivation of FFT sub-blocks on the receiver side than the deactivation of IFFT sub-blocks. This is due to the fact that the deactivation of larger FFT blocks than those corresponding to the selected R value, leads to information loss because some FFT blocks with non-identical inputs are assumed to have zero outputs. The size of the IFFT block that can be deactivated, depends only on the sparseness level S of the input data because the IFFT deactivation was based on the assumption that almost all of the input symbols X_k with odd-k, have an identical value X_c.

The simulation of an OFDM environment with AWGN channel noise showed that the use of the proposed sub-sampling technique can lead to full information recovery if the input data are sparse enough (S=0.5%) and the number of samples R that are omitted and replaced by others is below N/16 for the case of N=1024 and 16-QAM modulation. If S is higher (2%), a full information recovery is still possible at higher channel SNR. In 4-QAM modulation (QPSK) and N=256, full reconstruction was achieved in all the cases that have been tested with S=0.5%. A BER below 10^{-3} instead of a full reconstruction can be achieved in all cases if S=2%. The deactivation of FFT sub-blocks that accept as input the samples that have already replaced by others does not affect the error at all, as expected. However, even if larger number of operations (N/2 of the FFT or IFFT) is skipped and R=N/8 of the samples are replaced, then the effect on the BER is negligible since it increases from approximately 10^{-5} to 10^{-4} in the worst case as shown in Fig. 9 (S=0.5%).

Several image (with S between 5% and 10%) reconstruction examples have also been tested with the system configurations examined above (not presented in detail due to lack of space). The maximum NMSE that appeared in these cases was in the order of 10^{-4}. Comparing the NMSE error and the BER measurements of this work with the ones referenced in Section I, it can be stated that a higher precision is achieved with the proposed method than many other approaches although the number of samples needed is higher. The most important advantage of this work is that it can be implemented with very low cost hardware.

VI. Conclusions

An OFDM environment with sub-sampling support was described in this paper. The sub-sampling mode can last up to ¾ of the time saving power, memory and increasing the speed. Although the information on the receiver side was recovered using fewer samples, a signal reconstruction with very low or no error at all was possible. The proposed method can be implemented with very low complexity hardware. The proposed OFDM system will be implemented on real hardware and is expected to occupy the same number of resources with an ordinary OFDM transceiver.

References

[1] N. Petrellis, "Under-sampling in OFDM Telecommunication Systems," MDPI Applied Sciences Vol. 4, No 1, pp. 79-98, 2014.

[2] N. Petrellis, "Low Power OFDM Receiver Exploiting Data Sparseness and DFT Symmetry," Hindawi International Journal of Distributed Sensor Networks Vol. 2016, article id. 1464639, 2016.

[3] E.J. Candès, M.B. Wakin, An Introduction To Compressive Sampling," IEEE Signal Processing Magazine Vol 25, No 2, pp. 25-30, 2008.

[4] D.L. Donoho, "Compressed Sensing," IEEE Trans. On Information Theory Vol 52 No 4, pp. 1289-1306., 2006.

[5] J.L. Stanislaus, T. Mohsenin, "Low-complexity FPGA implementation of compressive sensing reconstruction," Proc. IEEE ICNC. 2013.

[6] Y.M. Tsai et al, "A Chip Architecture for Compressive Sensing Based Detection of IC Trojans," Proc. of the IEEE SiPS. 2012.

[7] A. Mahalanobis, R. Muise, "Object Specific Image Reconstruction using a Compressive Sensing Architecture for Application in Surveillance Systems," IEEE Trans. On Aerospace and Electronic Systems Vol 45, No 3, pp. 1167-1180, 2009.

[8] K. Tian, J. Wu, "A Review on Face Recognition Based On Compressive Sensing," IETE Technical Review, Vol. 30, No. 5, 2013.

[9] L. Xu, Q. Liang, "Compressive Sensing in Radar Sensor Networks Using Pulse Compression Waveforms," Proc IEEE ICC 2012.

[10] F. Fazel, M. Fazel, M. Stojanovic, "Random Access Compressed Sensing of Energy-Efficient Underwater Sensor Networks," IEEE Journal on Selected Areas in Communications, Vol 29, No 8, pp. 1660-1670, 2011.

[11] N. Vaswani, "Kalman filtered compressed sensing," Proc. 15th IEEE ICIP 2008.

[12] N. Vaswani, "Compressive Sensing on Least Squares Residual," IEEE Trans. Signal Processing Vol 58, No 8, pp. 4108-4120, 2010.

[13] A. Carmi, P. Gurfil, D. Kanevsky, "Methods for Sparse Signal Recovery Using Kalman Filtering With Embedded Pseudo-Measurement Norms and Quasi-Norms," IEEE Trans. Sig. Proc. Vol 58, No 4, pp. 2405-2409, 2010.

[14] A. Hormati, M. Vetterli. "Compressive Sampling of Multiple Sparse Signals Having Common Support Using Finite Rate of Innovation Principles," IEEE Signal Processing Letters. Vol. 18, No 5, pp. 331-334, 2011

[15] C. Qi, L. Wu, "A Hybrid Compressed Sensing Algorithm for Sparse Channel Estimation in MIMO OFDM Systems," Proc. IEEE ICASSP, 2011.

[16] P. Poshalla. Why Oversampling When Undersampling Can Do the Job. Texas Instruments Application Report 2013. Available: http://www.ti.com/lit/an/slaa594a/slaa594a.pdf

[17] C. Pimentel, R. Demo Souza, B.F. Uchoa-Filho, I. Benchimol. "Minimal trellis for systematic recursive convolutional encoders," Proc. IEEE ISIT. 2011.

[18] J.W. Cooley, J.W. Tukey, "An Algorithm for the Machine Calculation of Complex Fourier Series," Mathematical Computer Vol 19, pp. 297-301, 1965.